LIBYAN JOURNAL OF MEDICINE
2021, VOL. 16, 1883224
https://doi.org/10.1080/19932820.2021.1883224

Taylor & Francis
Taylor & Francis Group

ORIGINAL ARTICLE

Corylin suppresses metastasis of breast cancer cells by modulating miR-34c/LINC00963 target

Shourong Liu[a], Li Wang[b] and Run Zhang[c]

[a]Department of Oncology and Hematology, Luzhou People's Hospital, Luzhou, China; [b]Hemodialysis Center, Jiangmen Wuyi Hospital of Traditional Chinese Medicine, Jiangmen, China; [c]Department of Nursing, Luzhou People's Hospital, Luzhou, China

ABSTRACT

Breast cancer is one of the cancers leading to most death cases among women and metastasis is the major cause of breast cancer mortality. In this study, Corylin, the flavonoid compound which is extracted and purified from *Psoralea corylifolia* L., the effect on breast cancer metastasis was investigated. Corylin showed inhibitory effect on migration and invasion abilities of breast cancer cells. Meanwhile, the epithelial–mesenchymal transition was also regulated by corylin. The long non-coding RNA LINC00963 was found to have a significantly high expression level in breast cancer while it can be down-regulated by corylin. In addition, both wound-healing assay and transwell assay showed that LINC00963 induced breast cancer cells metastasis. MiR-34c was increased by corylin treatment depending on p53, and it was firstly identified that the LINC00963 was a direct target of miR-34c. Corylin was verified here that it prohibited MCF-7 migration and invasion depending on miR-34c/LINC00963 target. In conclusion, corylin suppresses metastasis of breast cancer cells via increasing miR-34c expression, which was dependent on p53. LINC00963 was a direct target of miR-34c and the target axis was necessary for corylin function. Therefore, corylin is a promising drug candidate and LINC00963 can be seen as a promising target in breast cancer treatment

ARTICLE HISTORY
Received 28 December 2020
Accepted 26 January 2021

KEYWORDS
Corylin; LINC00963; miR-34c; breast cancer; metastasis

1. Introduction

Breast cancer is one of cancers leading to most death cases among women. The incidence of breast cancer is increasing by 0.3% every year [1,2]. Metastasis is the major cause of mortality for breast cancer as the primary tumor migrates to remote organs including lung, liver, and bone [3]. Studies on metastasis molecular mechanisms has improved therapeutic strategies. Epithelial-mesenchymal transition (EMT) is an essential and reversible process in breast cancer metastasis that polarized epithelial cells to become mesenchymal cells with loosening cell-cell adhesion junctions [4]. Thus, understanding EMT mechanisms is promising for looking for early biomarkers contributing to treatment.

Corylin is a type of flavonoid compound, which is extracted and purified from *Psoralea corylifolia* L. (Fabaceae) [5]. The herb is commonly used as Traditional Chinese Medicine for treatments of different diseases such as cardiovascular diseases [6] and osteoporosis [7]. Among natural products from *P. corylifolia* L., corylin is the main flavonoid and shows several therapeutic effects such as anti-inflammation, anti-oxidation, and anti-cancers for hepatocellular carcinoma [5]. However, the function of corylin on breast cancer is still unknown. It is provoking and intriguing to investigate the detailed effects and mechanisms of corylin on breast cancer. The study will provide the possible drug candidate for breast cancer treatment.

Long non-coding RNA (lncRNA) is a type of RNAs containing over 200 nucleic acids and does not encore functional proteins [8]. In whole human genome, lncRNAs take part more than 50% of all transcripts. Recently, different researches revealed that lncRNAs play important roles in variety of diseases progress [9,10]. LINC00963 is a novel long non-coding RNA locating on chromosome 9 with around 2.1 kb in length. Several effects of LINC00963 on different cancers were investigated in previous studies. In hepatocellular carcinoma, PI3K/AKT signaling pathway was activated by LINC00963 [11]. It was also reported that LINC00963 promoted ovarian cancer proliferation and its expression level increased in esophageal squamous cell carcinoma, while knockdown of LINC00963 inhibited the growth of esophageal squamous cell carcinoma *in vitro* and *in vivo* [12,13]. Therefore, in current study, the regulatory relationships between corylin and LINC00963 will be investigated. Furthermore, the target between LINC00963 and miR-34c was also validated. It is the first research connecting corylin effect and LINC00963/miR-34c target. This study will provide a novel potential target and drug candidate for breast cancer treatment.

CONTACT Run Zhang Luzhou People's Hospital, No.316 Jiugu Avenue, Luzhou 646000, China runzhang_lzph@yahoo.com

2. Materials and methods

2.1. Materials

Corylin (PHL83287) was purchased from Sigma-Aldrich. The specific p53 siRNA was designed and synthesized by Sangon (Shanghai, China). All cell culture stuffs including 6-well plates, T75 flasks were purchased from Corning (USA). The primary antibodies against Vimentin, SNAI1, E-cadherin and p53 were purchased from Abcam (USA). The xCELLigence system was obtained from Agilent (USA). SYBR Green mix for q-PCR was purchased from QIAGEN (Germany).

2.2. Cell culture and treatment

MCF-7 and MDA-MB-231 cells were purchased from ATCC. Dulbecco's Modified Eagle Medium (DMEM) and RPMI-1640 medium (Gibco, USA) were used for MCF-7 and MDA-MB-231 culturing, respectively, containing 10% FBS (Gibco, USA). The culturing condition is 37°C, 5% CO2. For different experiments, cells were seeded in 6-well plates and then treated with corylin in variety of concentrations (0, 2.5, 5, 10, 15, 20 μM) for 24 hours.

2.3. Vector cloning

LINC00963 harboring miR-34c binding site and p53 coding sequence (CDS) were amplified using polymerase chain reaction (PCR) from human cDNA templates. Obtained LINC00963 was confirmed through by Sanger sequencing. The primers used were as follow (5′ → 3′):

LINC00963

Forward: 5′CCGGCCCGTCTCGGGGCCCTGA3′

Reverse: 5′TTTTTTATGCTGAAAATATTCCAAGGTTTATTG3′

P53 CDS

Forward: 5′CGTGCTTTCCACGACGGTGACACGCTTCCCTGG3′

Reverse: 5′TTTGGCAGCAAAGTTTTATTGTAAAATAAGAGATC3′

LINC00963 and p53 PCR product (named as pcD-LINC00963 and pcD-p53 respectively) was cloned into pcDNA3.1 (+) vector (Ambion, Austin, USA) and the constructs were confirmed through Sanger sequencing. LINC00963 wild type and mutant type pGL-3 reporter plasmid (Promega, USA) were constructed and contained the sequences of miR-34c binding site or mutant site.

2.4. Transfection

To transfect p53 siRNA or miR-34c mimics/negative control, cells were seeded into 6-well plates at density of 5×10^4 cells/well. Transfection was conducted when cell confluence reached more than 70%. The final concentration of siRNA or miRNA is 25 nM and Lipofectamine 2000 (Life, USA) was employed according to product instruction. In this study, the ratio of RNA and Lipofectamine 2000 was 1:2. After mixing RNAs and Lipofectamine 2000 in Opti-MEM (Gibco, USA), incubated the mixture for 5 min at room temperature. Then, mixtures were added into cells dropwisely. A universal negative control siRNA (siRNA NC) or a negative control was used.

2.5. Quantitative real time PCR (q-PCR)

Total RNA isolation was performed with High Pure RNA Isolation Kit (Roche, Switzerland). Then cDNA library was established through total RNA reverse transcription with verso cDNA Synthesis Kit (Thermo Fisher, USA) based on the product instruction. SYBR™ Green PCR Master Mix (Thermo Fisher, USA) was used for q-PCR test, and results were calculated with $2^{-\Delta\Delta CT}$ of each group. The PCR reaction conditions were as follows: 95°C for 15 s followed by 40 cycles of 95°C for 5 s and 60°C for 30s. The gene expression levels for miRNA and protein genes were normalized to U6 RNA and glyceraldehyde-3-phosphate dehydrogenase (GAPDH) expressions respectively. Primers of each tested gene are listed below (5′ to 3′):

Vimentin

Forward: 5′AGTCCACTGAGTACCGGAGAC3′

Reverse: 5′CATTTCACGCATCTGGCGTTC3′

SNAI1

Forward: 5′TCGGAAGCCTAACTACAGCGA3′

Reverse: 5′AGATGAGCATTGGCAGCGAG3′

CDH1

Forward: 5′AAAGGCCCATTTCCTAAAAACCT3′

Reverse: 5′TGCGTTCTCTATCCAGAGGCT3′

LINC00963

Forward: 5′GTCAGGCCACTCTGCTACTG3′

Reverse: 5′CAACTGCGATGGTTGTGCTC3′

2.6. Western blot

Detailed procedure of western blot was described elsewhere. Briefly, after different treatments, cells were lysed with RIPA buffer and quantified by using BCA kit based on product protocol. For gel electrophoresis, 30 μg protein samples were loaded and separated by 10% sodium dodecyl sulfate polyacrylamide gel. After electrophoresis, protein was transferred to polyvinylidene fluoride (PVDF) membranes. primary antibodies were diluted into 1 x TBST in 5% BSA, and incubated with PVDF membranes over night at 4°C or 1 h at 37°C. The used primary antibodies were: Vimentin (1:1000, abcam, USA), SNAI1 (1:1000, Santacruz, USA), E-Cadherin (1:1000, abcam), p53 (1:1000, Cell signaling Technology, USA) and β-actin (1:2000, abcam, USA).

Secondary antibodies were diluted into 5% skim milk in 1 x TBST (1:10,000) and incubated for 1 h at room temperature. Enhanced chemiluminescence (ECL) system was employed for imaging.

2.7. Wound-healing assay

Cells were treated with different concentrations of corylin 24 h before being seeded into 6-well-plate at density of 5×10^5 cells/well. After seeding into 6-well plate and culturing overnight, the wound was generated with 10 µl tips and then rinsed twice with warmed PBS to wash cell debris. Next, incubated cells for 1 h and take pictures with microscope to obtain migration distance (D0) at 0 h. After 24 h incubation, wounds were imaged again and recorded migration distance (Dt). The following formula was used to calculate migration rate: migration rate (%) = (Dt − D0)/D0 x 100%.

2.8. Transwell assay

Cells were treated with different concentrations of corylin 24 h before being seeded into 8 µm transwell chamber at density of 3×10^5 cells/well. The FBS concentration in lower chamber was 15%. After seeding and culturing for 48 h, cells were fixed with methanol for 30 min and then stained with 0.5% crystal violet for 20 min. Chambers were washed three times with PBS and removed cells in upper chambers gently. Cell images were obtained through microscope and quantified by counting cell numbers.

2.9. Luciferase assay

The 3′- untranslated regions (3′UTRs) of LINC00963 containing wild type or mutant binding sites for miR-34c were cloned into pGL3 control vector. HEK-293 T cells were used to be co-transfected with reporter vector and miRNA. HEK-293 T cells were seeded in a 12-well plate at 2×10^4 cells/well and transfected with 100 ng reporter vector and 20 ng Renilla reporter plasmid as a normalization control. After incubated for 72 h, Luciferase activities of each group were tested by Orion II luminometer (Berthold, Bad Wildbad, Germany) in 96-well plate and analyzed with the SIMPLICITY software package (DLR, Stuttgart, Germany).

2.10. Statistics

All data are presented as mean ± SD values. Two different groups comparisons were analyzed by Student's t-test. TCGA sample analysis with multiple groups were achieved by one-way analysis of variance (one-way ANOVA) and followed by a Tukey multiple comparisons post-hoc test. P values of < 0.05 (*p) or < 0.01 (**p) were considered statistically significantly different.

3. Results

3.1. Corylin suppressed migration and invasion ability of breast cancer cells

To test the potential therapeutic effect of corylin on breast cancer, two breast cancer cell lines MCF-7 and MDA-MB-231 were selected for corylin treatment with different concentrations (0–200 µM). The results from xCELLigence real-time cell analyzer showed that corylin inhibited proliferation rates of both MCF-7 and MDA-MB-231 cells in each used concentration compared to untreated group (Figures 1A and Figure 1B). In addition, high concentration exhibited stronger inhibitory ability on cell proliferation, which indicates that the effect of corylin on proliferation was dosage-dependent. The IC50 of corylin on MCF-7 and MDA-MB-231 were 10.58 µM and 13.59 µM, respectively, calculated by GraphPad Prism 8. Next, the effect of 10 µM corylin on migration and invasion ability were tested through wound-healing assay and transwell assay, respectively. As shown in Figures 1C and Figure 1D, corylin significantly suppressed migration of MCF-7 and MDA-MB-231 compared with control group. Meanwhile, the invasion ability was also inhibited by corylin treatment in two breast cancer cell lines (Figure 1E).

3.2. Corylin inhibited Epithelial-Mesenchymal Transition (EMT)

Epithelial-mesenchymal transition (EMT) plays key role in tumor metastasis as adhesions among cells were weaken and migrate to remote sites. Here several EMT-associated proteins and genes were tested by western blot and q-PCR after treated with corylin. As shown in Figure 2A, EMT promoting proteins including Vimentin and SNAI1 decreased after corylin treatment while epithelial marker E-cadherin increased compared with control group in both MCF-7 and MDA-MB-231 cells. In q-PCR results from both cell lines, corylin treatment also inhibited Vimentin and SNAI1 gene expression and increased CDH1 expression (Figures 2B and Figure 2C).

3.3. Corylin induced miR-34c in breast cancer cells

In order to further investigate the detailed molecular mechanism of corylin function, miRNAs expression profile was analyzed from GEO datasets (GSE16477). Briefly, total 127 miRNAs were up-regulated and 48 miRNAs were down-regulated in MCF-7 cell (Figure 3A), 117 miRNAs were up-regulated and 63 miRNAs were down-regulated

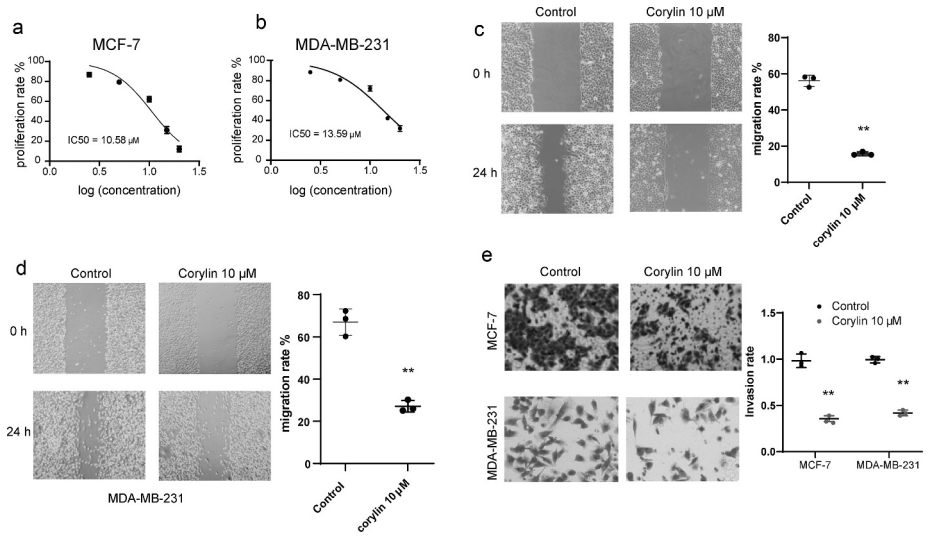

Figure 1. The effect of corylin with different concentrations on proliferation rate of MCF-7 (A) and MDA-MB-231 cells (B). The IC50 of corylin for MCF-7 and MDA-MB-231 are 10.58 μM and 13.59 μM respectively. (C) Migration ability of MCF-7 was measured by wound-healing assay. 10 μM corylin inhibited migration ability compared with control group (**p < 0.01). (D) Migration ability of MDA-MB-231 was measured by wound-healing assay. 10 μM corylin inhibited migration ability compared with control group (**p < 0.01). (E) Invasion abilities of MCF-7 and MDA-MB-231 were measured by traswell assay. 10 μM corylin inhibited invasion ability compared with control group (**p < 0.01).

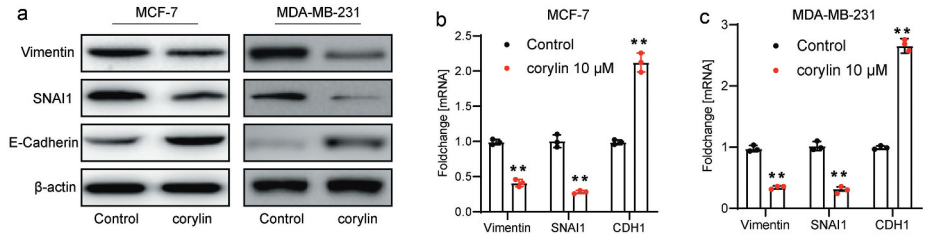

Figure 2. (A) EMT markers' protein level was tested by western blot. In both MCF-7 and MDA-MB-231 cells, 10 μM corylin inhibited Vimentin and SNAI1 and induced E-cadherin compared with control group. EMT markers gene expression was tested by q-PCR. In both MCF-7 (B) and MDA-MB-231 cells (C), corylin inhibited Vimentin and SNAI1 and induced CDH1 expression compared with control group (**p < 0.01).

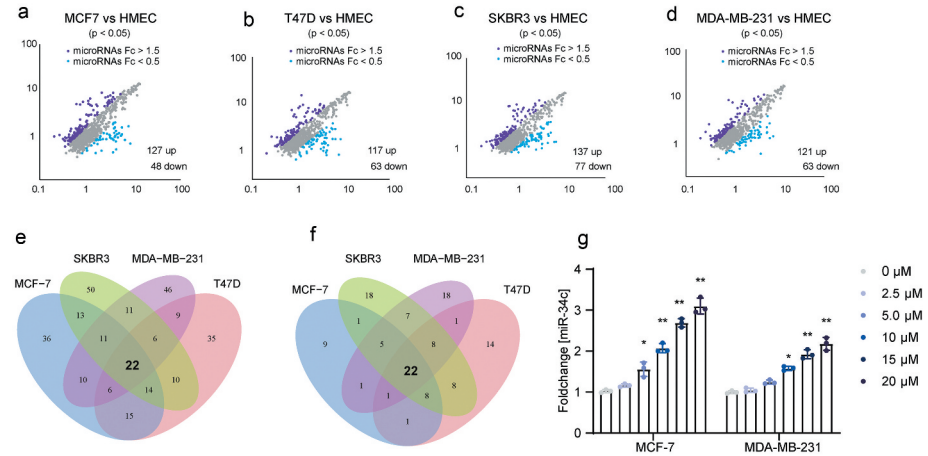

Figure 3. GEO data sets GSE16477 was analyzed. Differential expressed microRNAs (Fc > 1.5 or Fc < 0.5) were presented after comparing MCF-7 (A), T47D (B), SKBR3 (C) or MDA-MB-231 (D) to HMEC cells. (E) In all up-regulated microRNAs (Fc > 1.5), there are 22 common up-regulated microRNAs when compared MCF-7, SKBR3, T47D and SKBR3. (F) In all down-regulated microRNAs (Fc < 0.5), there are 22 common down-regulated microRNAs when compared MCF-7, SKBR3, T47D and SKBR3. (G) The effect of corylin with different concentrations on miR-34c expression of MCF-7 and MDA-MB-231 cells. Corylin increased miR-34c expression which is concentration dependent (*p < 0.05, **p < 0.01).

in T47D cell (Figure 3B), 137 miRNAs were up-regulated and 77 miRNAs were down-regulated in SKBR3 cell (Figure 3C), 121 miRNAs were up-regulated and 63 miRNAs were down-regulated in MDA-MB-231 cell (Figure 3D). Then the common up-regulated or down-regulated miRNAs were compared among those four breast cancer cell lines. Total 22 up-regulated miRNAs and 22 down-regulated miRNAs were obtained and selected for further study (Figure 3E, Figure 3F and Table 1). Next, all chosen miRNAs were validated by q-PCR in MCF-7 and MDA-MB-231 cells (data not shown). As shown in Figure 3G, only miR-34c was found to be increased significantly after corylin treatment. Therefore, miR-34c was a promising candidate in further molecular mechanism research.

3.4. P53 was required for miR-34c induction by corylin

Since all miR-34 family members (miR-34a, miR-34b/c) are induced by p53, in next step, the potential role of p53 in corylin function was investigated. In MCF-7 (p53 wild genotype), p53 was knocked down by specific siRNA (Figure 4A). After p53 knocking down, the induction effect of corylin on miR-34c was partly abolished (Figure 4B). Similarly, in MDA-MB-231 cell harboring mutant p53, ectopically expressed p53 (Figure 4A) further induced miR-34c expression after corylin treatment compared to corylin treatment only (Figure 4C). In conclusion, miR-34c can be increased by corylin partly dependent on p53 status.

Table 1. Common up- and down-regulated miRNAs in four cell lines (GSE16477).

Up-regulated miRNAs	Down-regulated miRNAs
hsa-miR-7	hsa-miR-3180-2
hsa-miR-1244	hsa-miR-485
hsa-miR-219-5p	hsa-miR-3180-3
hsa-miR-1972	hsa-miR-1909
hsa-miR-1255b	hsa-miR-3181
hsa-miR-1303	hsa-miR-376a
hsa-miR-484	hsa-miR-3188
hsa-miR-519a*	hsa-miR-2116
hsa-miR-1283-1	hsa-miR-3180-1
hsa-miR-4305	hsa-miR-409
hsa-miR-25	hsa-miR-382
hsa-miR-1302-8	hsa-miR-1202
hsa-miR-1300	hsa-miR-572
hsa-miR-23b	hsa-miR-874
hsa-miR-27b	hsa-miR-718
hsa-miR-15b	hsa-miR-939
hsa-miR-4302	hsa-miR-4322
hsa-miR-514-1	hsa-miR-1271
hsa-miR-4315-2	hsa-miR-22
hsa-miR-520d	hsa-miR-3195
hsa-miR-2054	hsa-miR-34 c
hsa-miR-3165	hsa-miR-31

3.5. LINC00963 induced migration and invasion ability of breast cancer cells

To further investigate the potential genes regulated by corylin and targeted by miR-34 c, the gene expressions profiles including both coding and non-coding RNAs from TCGA database were analyzed. Of note, there were total 1643 genes up-regulated with fold change (Fc) over 2.0 and 1966 genes down-regulated with Fc less than 0.5 (Figure 5A). Among those top 200 up-regulated genes, LINC00963 was predicted as a miR-34 c target according to ENCORI and it was never studied before (Figure 5B). Next, LINC00963 was evaluated by q-PCR after transfected with miR-34c mimics. As shown in Figure 5C, the long non-coding RNA LINC00963 was a promising target of miR-34c as its mRNA expression was reduced by miR-34c mimics. Then, the function of LINC00963 on EMT was tested. LINC00963 overexpression (Figure 5D) induced mesenchymal marker protein level and inhibited epithelial marker in MCF-7 cells (Figure 5E). In addition, LINC00963 was also observed to have similar effect on EMT markers mRNA when tested by q-PCR (Figure 5F).

3.6. Corylin function was dependent on miR-34c/LINC00963 target

In order to confirm the direct target between miR-34c and LINC00963, the sequences fragment of LINC00963 harboring wild/mutant seeds (pGL3-linc-WT/pGL3-linc-MUT) were cloned into pGL3 Luciferase Reporter System (Figure

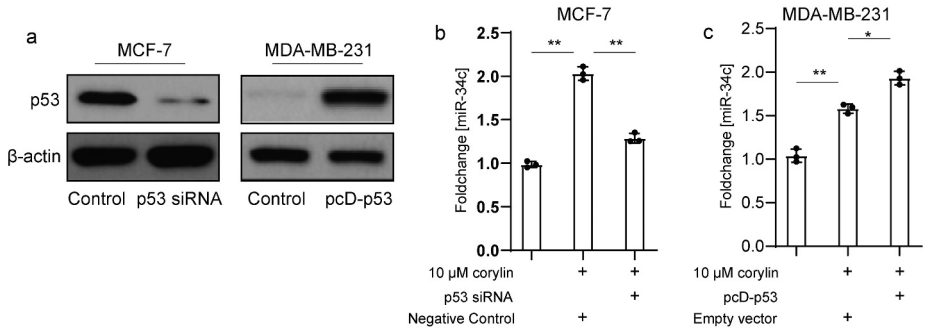

Figure 4. (A) In MCF-7 cell, p53 specific siRNA inhibited p53 protein level while overexpression plasmid pcD-p53 increased p53 protein level in MDA-MB-231 cells. (B) In MCF-7 cells, p53 knocking down by siRNA reversed the effect of corylin on inducing miR-34c compared with negative control (**p < 0.01). (C) In MDA-MB-231 cells, p53 rescuing by pcD-p53 further enhanced the effect of corylin on inducing miR-34c compared with empty vector (**p < 0.01).

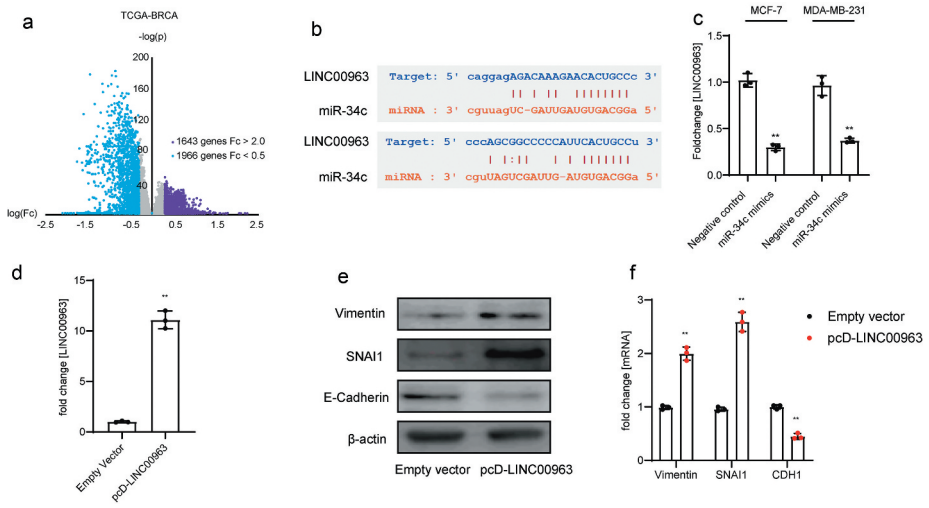

Figure 5. (A) TCGA-BRCA data was analyzed. In BRCA tissue, there are total 1643 genes up-regulated with fold change over 2.0 while 1966 genes down-regulated with fold change less than 0.5 when compared with normal tissue. (B) LINC00963 was predicted that there are miR-34 c targets on its sequences obtained from online bioinformatic tool ENCORI. (C) In both MCF-7 and MDA-MB-231 cells, transfected miR-34 c mimics significantly decreased LINC00963 expression (**p < 0.01). (D) In MCF-7 cell, the ectopically expressed LINC00963 was achieved by pcD-LINC00963 (**p < 0.01). (E) In MCF-7 cell, overexpression of LINC00963 increased Vimentin and SNAI1 protein level while inhibited E-cadherin protein. (F) In MCF-7 cells, overexpression of LINC00963 increased Vimentin and SNAI1 mRNA level while inhibited CDH1 expression (**p < 0.01).

6A). As predicted, miR-34c mimics significantly suppressed the luciferase activity in pGL3-linc-WT group compared to pGL3-linc-MUT group, suggesting that LINC00963 was a direct target of miR-34c (Figure 6B). Next, whether the corylin function was dependent on miR-34c/LINC00963 target was verified. In MCF-7, corylin treatment decreased LINC00963 expression (Figure 6C) while overexpression LINC00963 abolished the inhibitory effect of corylin on cell migration (Figure 6D) and invasion (Figure 6E). Furthermore, miR-34c was still induced by corylin in MCF-7 when cells were ectopically expressed with LINC00963 (Figure 6F)(Figure 6A).

4. Discussion

Corylin, one of the main flavonoids isolated from *Psoralea corylifolia* L., has been demonstrated to exhibit various biological properties such as anti-tumor and anti-inflammatory effects [5,7]. However, the effect of corylin on breast cancer metastasis and the detail molecular mechanisms are still unclear. In this study, corylin showed inhibitory effect on migration and invasion ability of breast cancer cells. Meanwhile, the epithelial–mesenchymal transition (EMT) was also regulated by corylin. After corylin treatment, mesenchymal markers such as Vimentin and SNAI1 were decreased while epithelial markers E-cadherin was increased. Therefore, it is reasonable for the explanation that corylin inhibits metastasis through affecting EMT.

Emerging evidence illustrated that long non-coding RNAs can participate in different diseases progresses including different cancers [8]. Interacting with microRNAs is one of the main ways how lncRNAs play the role. In previous studies, lncRNA LINC00963 has been identified to exhibit tumor-promoting effects in several cancer types. In acute myeloid leukemia, cancer development was facilitated by LINC00963 through modulating miR-608/MMP-15 targeting [14]. Furthermore, LINC00963 was significantly increased in colorectal cancer tissues and cells, and LINC00963 promoted colorectal cancer proliferation and migration through direct target of miR-124-3p related to FZD4 [15]. LINC00963 also conferred oncogenic properties in bladder cancer as high LINC00963 expression was observed in bladder cancer patients and indicated high histological grade. Bladder cancer cells viability, colony formation, migration, and invasion can be suppressed by LINC00963 knocking down [16]. In our study, LINC00963 was found to have a significant high expression level in breast cancer patients in TCGA database. In addition, both wound-healing assay and transwell assay showed that LINC00963 induced breast cancer cell metastasis. When breast cancer cells were treated with corylin, LINC00963 was significantly reduced. According to the results of migration and invasion abilities measurements, LINC00963 abolished the inhibitory effect of corylin. Results above indicated that LINC00963 was one of the effectors of corylin, which means corylin inhibited breast cancer cells metastasis through regulating LINC00963.

Furthermore, the p53 induced microRNA miR-34c was up-regulated in corylin treatment group. Tremendous evidence suggested that miR-34 family played tumor-suppressing role [17]. miR-34 family contains miR-34a encoded in the second exon of a gene located on chromosome 1p36.22, and miR-34b/c share common host gene located on chromosome 11q23.1. In multiple cancer types, miR-34s inhibit tumor growth, metastasis, and proliferation via affecting cellular processes including

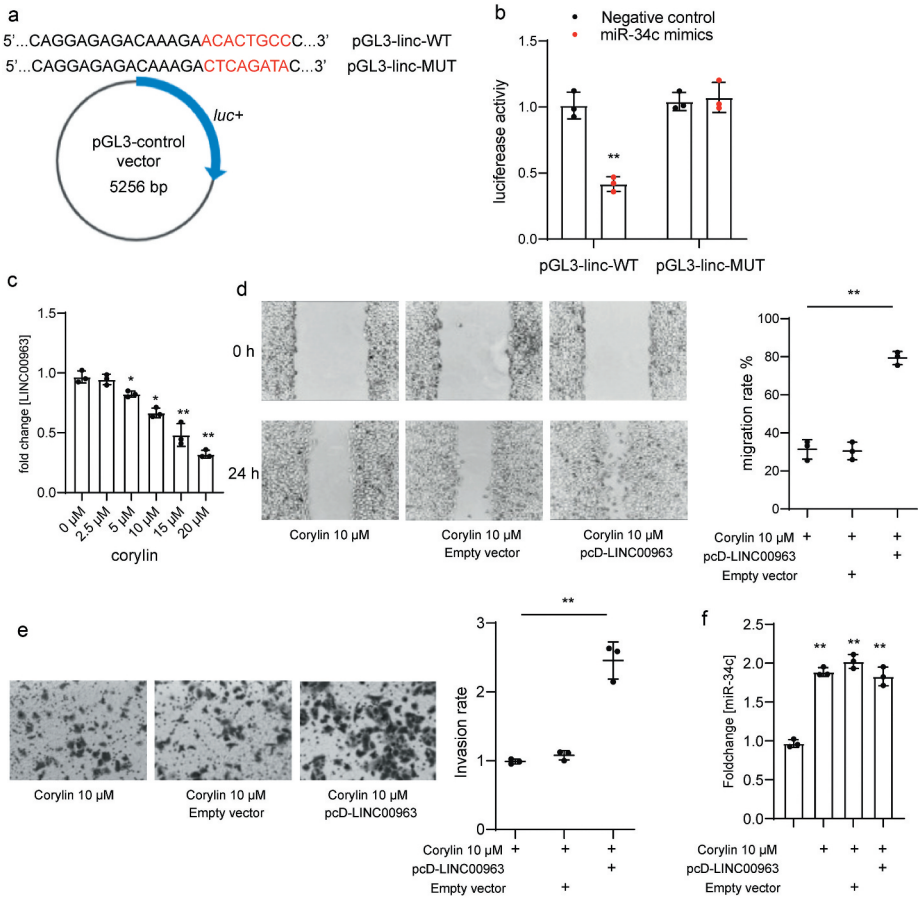

Figure 6. (A) Luciferase system pGL3-linc-WT and pGL3-linc-MUT containing wild type or mutant type of seed sequences were constructed. (B) In luciferase assay, miR-34c mimics significantly suppressed luciferase activity of pGL3-linc-WT when compared to negative control (**p < 0.01). (C) In MCF-7 cell, Corylin inhibited LINC00963 expression which is concentration dependent tested by q-PCR (*p < 0.05, **p < 0.01). (D) In wound-healing assay, overexpression of LINC00963 reversed the inhibitory effect of corylin on MCF-7 migration activity (**p < 0.01). (E) In transwell assay, overexpression of LINC00963 reversed the inhibitory effect of corylin on MCF-7 invasion activity (**p < 0.01). (F) Overexpression of LINC00963 cannot reverse the miR-34c expression induced by corylin (**p < 0.01).

cell cycle, EMT, and stemness [18]. In our study, miR-34c was characterized to be down-regulated in four different breast cancer cell lines and was increased by corylin treatment in MCF-7 and MDA-MB-231 cells. In addition, p53 was required for the function of corylin on regulating miR-34 c since silencing p53 abolished the effect of corylin on inducing miR-34c. In this study, we firstly identified that the lncRNA LINC00963 was a direct target of miR-34c. Ectopic expression of miR-34c decreased LINC00963 in both MCF-7 and MDA-MB-231 cells. Considering miR-34c was induced by corylin treatment, the target between miR-34 c and LINC00963 suggests that corylin inhibits breast cancer cell metastasis through increasing miR-34c which leads to LINC00963 degrading. Interestingly, overexpression of LINC00963 cannot affect miR-34c induced by corylin, which implies that corylin suppressed LINC00963 through miR-34c targeting but LINC00963 never showed sponge ability to miR-34 c. Therefore, miR-34c locates on upstream of LINC00963 in the whole regulation axis regulated by corylin.

In conclusion, corylin suppresses metastasis of breast cancer cells via increasing miR-34c expression, which is dependent on p53. LINC00963 is a direct target of miR-34c and the target axis is necessary for corylin function. Corylin is a promising drug candidate and LINC00963 can be seen as a promising target in breast cancer treatment.

Acknowledgments

None.

Disclosure statement

No potential conflict of interest was reported by the authors.

References

[1] Scott AR, Stoltzfus KC, Tchelebi LT, et al. Trends in cancer incidence in US adolescents and young adults, 1973-2015. JAMA Network Open. 2020;3(12):e2027738. .

[2] Siegel RL, Miller KD, Jemal A. Cancer statistics, 2018. CA Cancer J Clin. 2018;68(1):7–30.

[3] Chaffer CL, Weinberg RA. A perspective on cancer cell metastasis. Science. 2011;331(6024):1559–1564.
[4] Lambert AW, Pattabiraman DR, Weinberg RA. Emerging biological principles of metastasis. Cell. 2017;168 (4):670–691.
[5] Chen CY, Chen CC, Shieh TM, et al. Corylin suppresses hepatocellular carcinoma progression via the inhibition of epithelial-mesenchymal transition, mediated by long noncoding RNA GAS5. Int J Mol Sci. 2018;19(2):380.
[6] Chen CC, Li HY, Leu YL, et al. Corylin inhibits vascular cell inflammation, proliferation and migration and reduces atherosclerosis in ApoE-Deficient mice. Antioxidants (Basel). 2020;9(4):275.
[7] Yu AX, Xu ML, Yao P, et al. Corylin, a flavonoid derived from Psoralea Fructus, induces osteoblastic differentiation via estrogen and Wnt/beta-catenin signaling pathways. Faseb J. 2020;34(3):4311–4328.
[8] Gibb EA, Brown CJ, Lam WL. The functional role of long non-coding RNA in human carcinomas. Mol Cancer. 2011;10(1):38.
[9] Meng J, Li P, Zhang Q, et al. A four-long non-coding RNA signature in predicting breast cancer survival. J Exp Clin Cancer Res. 2014;33(1):84.
[10] Serviss JT, Johnsson P, Grander D. An emerging role for long non-coding RNAs in cancer metastasis. Front Genet. 2014;5:234.
[11] Wu JH, Tian XY, An QM, et al. LINC00963 promotes hepatocellular carcinoma progression by activating PI3K/AKT pathway. Eur Rev Med Pharmacol Sci. 2018;22 (6):1645–1652.
[12] Liu W, Yang YJ, An Q. LINC00963 promotes ovarian cancer proliferation, migration and EMT via the miR-378g/CHI3L1 axis. Cancer Manag Res. 2020;12:463–473.
[13] Liu HF, Zhen Q, Fan YK. LINC00963 predicts poor prognosis and promotes esophageal cancer cells invasion via targeting miR-214-5p/RAB14 axis. Eur Rev Med Pharmacol Sci. 2020;24(1):164–173.
[14] Zuo W, Zhou K, Deng M, et al. LINC00963 facilitates acute myeloid leukemia development by modulating miR-608/MMP-15. Aging (Albany NY). 2020;12(19):18970–18981.
[15] Zheng K, Zhang TK. LncRNA LINC00963 promotes proliferation and migration through the miR-124-3p/FZD4 pathway in colorectal cancer. Eur Rev Med Pharmacol Sci. 2020;24(14):7634–7644.
[16] Zhou N, Zhu X, Man L. LINC00963 functions as an oncogene in bladder cancer by regulating the miR-766-3p/MTA1 axis. Cancer Manag Res. 2020;12:3353–3361.
[17] Hermeking H. The miR-34 family in cancer and apoptosis. Cell Death Differ. 2010;17(2):193–199.
[18] Rokavec M, Li H, Jiang L, et al. The p53/miR-34 axis in development and disease. J Mol Cell Biol. 2014;6 (3):214–230.